General Disclaimer

One or more of the Following Statements may affect this Document

- This document has been reproduced from the best copy furnished by the organizational source. It is being released in the interest of making available as much information as possible.

- This document may contain data, which exceeds the sheet parameters. It was furnished in this condition by the organizational source and is the best copy available.

- This document may contain tone-on-tone or color graphs, charts and/or pictures, which have been reproduced in black and white.

- This document is paginated as submitted by the original source.

- Portions of this document are not fully legible due to the historical nature of some of the material. However, it is the best reproduction available from the original submission.

Produced by the NASA Center for Aerospace Information (CASI)
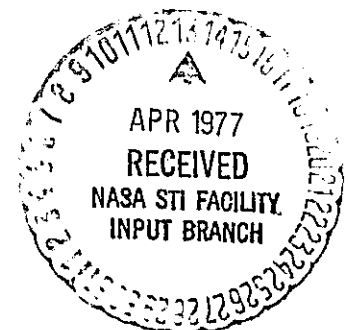
SUPERCONDUCTIVITY IN SPUTTERED CuMo$_6$S$_8$

by Samuel Alterovitz, John A. Woollam, Lee Kammerdiner,
Huey-Lin Luo, and Christopher Martin
Lewis Research Center
Cleveland, Ohio 44135

SUPERCONDUCTIVITY IN SPUTTERED CuMo$_6$S$_8$

by Samuel Alterovitz, John A. Woollam, Lee Kammerdiner,
Huey-Lin Luo, and Christopher Martin
Lewis Research Center
Cleveland, Ohio 44135

SUPERCONDUCTIVITY IN SPUTTERED $CuMo_6S_8$

by Samuel Alterovitz,[*] John A. Woollam, Lee Kammerdiner,[**]
Huey-Lin Luo,[**] and Christopher Martin,[***]

Lewis Research Center

INTRODUCTION

In 1971, Chevrel, et al. (ref. 1) discovered a new class of materials, now called "chevrel phases." These have the chemical formula M_xMo_6 (S or Se)$_8$, where M is any of a number of metals and x is variable. (Because of this formula we will call these compounds ternary molybdenum chalcogenides.) In the following year, Matthias, et al. (ref. 2) reported that many of these materials have high superconducting transition temperatures T_c. Odermat, et al. (ref. 3), reported superconducting upper critical fields, B_{c2}, above 50 tesla in materials with T_c's above 14 K, and Foner, et al. (refs. 4 and 5) reported B_{c2}'s above 60 tesla. By adding small amounts of rare earth metals Fisher, et al. (ref. 6) were able to observe 70 tesla B_{c2}'s in a lead-europium-gadolinium molybdenum sulfide. This is by far the highest superconducting B_{c2} ever reported. Fisher has reviewed some of the properties of the ternary molybdenum chalcogenides at the 14th International Conference on Low Temperature Physics (ref. 7) and at the Conference on the Physics of High Magnetic Fields in 1975 (ref. 8).

In all of the above work, samples were prepared by melting the metals, followed by annealing to various temperatures. The result was a structurally weak material. We have prepared and studied sputtered films on sapphire

---
[*]National Research Council Senior Research Associate.

[**]Department of Applied Physics and Information Sciences, University of California, San Diego.

[***]Winter Term student from Oberlin College, January 1977.

STAR category 76

substrates (ref. 9). The substrates give the films mechanical strength and permit easy attachment of electrical leads. We have also characterized the materials by x-ray diffraction, electron microscopy, electrical resistance vs. temperature, and B_{c2}, T_c, J_c (critical current) measurements. We present some of our results on $CuMo_6S_8$.

EXPERIMENTAL PROCEDURE

Samples were prepared (in duplicate) by sputtering, at the University of California, San Diego, where T_c and J_c's were measured in zero magnetic fields, and x-ray characterization was also done. Sputtering conditions were the same as described in reference 9 except that instead of forming the films at ambient temperatures and then annealing, the correct phase was formed directly by heating the substrates in the range of 600-800° C. The T_c's were measured in a differential transformer at 100 Hz. Duplicate samples were sent to NASA Lewis for high field studies. At NASA, T_c was measured inductively by a self inductance technique operating at about 100 kHz, and by d.c. electrical resistance methods. Temperatures were measured with carbon resistors (calibrated in fields), with germanium resistance thermometers, and with GaAs diodes. Calibrations were checked by measuring T_c onsets for pure indium and lead, and against the vapor pressure of liquid helium. Magnetic fields up to 14 tesla were generated in large bore superconducting solenoids. All critical field measurements were made with the field perpendicular to the plane of the samples and hence to the current. All critical current measurements were made with the field perpendicular to the current but parallel to the film. Film thickness measurement was a problem, but our most reliable measurements we believe were from use of a "profilometer," a device measuring the displacement of a needle dragged across the sample.

Two groups of samples were prepared. The basic reason which could account for the difference between group I and group II samples was that the substrate temperatures during deposition were generally lower for the

group II samples. This was consistent with the fact that group II samples showed broader x-ray diffraction peaks, higher resistivities and lower room temperature to T_c resistance ratios. Group I samples were thicker and wider than group II samples. From profilometer measurements of the films we get a thickness ranging from 0.6 μm to 1.0 μm within each sample in group II, and an approximate thickness of 1.7±.2 μm for group I samples. Critical currents were measured in samples from group II. Thicknesses varied from sample to sample, and within the same sample. In calculating J_c from I_c for group II samples, we used an effective thickness of 0.8 μm (by considering specific profiles) and a 1.7 mm width to calculate cross sectional areas. Scratches could present regions of greatly reduced thickness and could be missed by the profilometer. Thus the true effective thickness for J_c ($\equiv I_c$/area) calculations could be much smaller than the effective values used. Our J_c numbers thus represent a lower limit for these materials.

Experimental Results and Comparison With Theory

A. Critical Fields

Figure 1 presents data on B_{c2} vs. T_c in sample number 118 $CuMo_6S_8$ from group I. The resistive transition was defined as the midpoint between normal state resistance and zero resistance. Inductive transitions were taken as the onset of diamagnetism. A number of other samples were studied but will not be presented here.

Werthamer, Helfand, and Hohenberg (WHH) (ref. 10) have calculated the upper critical field, B_{c2}, as a function of temperature and the slope dB_{c2}/dT, including the effects of spin-orbit scattering and paramagnetic limiting. The assumptions of the theory are that the material is "dirty" ($l \ll \xi$ where l is the electron mean free path, and ξ is the coherence length) and that the time between spin flip collisions is long compared with non-spin flipping collision times. WHH also assume weak coupling (weak

electron-phonon interaction). We have used their expression relating B_{c2} to T_c to make computer generated plots of B_{c2} vs. T_c for various values of the Maki paramagnetic pair breaking parameter α, and the spin-orbit scattering parameter, λ_{so}.

Figure 1 has a plot of the WHH theory for $\lambda_{so} = \infty$, which gives the highest possible values of B_{c2} for this theory. Notice that the experimental points at low temperatures are above the theoretical curve by several percent. Experimental data were nearer to the $\lambda_{so} = \infty$ line for samples of group II (numbers 181, 191 (data not shown here). The WHH plot is very sensitive to the experimentally determined slope near T_c. The slope used for the plot in figure 1 was determined by matching the smoothed experimental data to WHH theory for reduced temperatures to between 0.7 and 1.0, where $t \equiv T/T_c$. This leads us to believe the experimental data for this sample are truly above the maximum WHH theoretical limit in the lower temperature range ($0 < t < 0.7$).

There are several possible reasons for this. WHH theory is for dirty, weak coupling materials with an isotropic Fermi surface. Any departure from these three assumptions will give a higher theoretical curve for $B_{c2}(T)$. A clean sample has a higher theoretical B_{c2} than a dirty one by as much as 5 percent (refs. 11 and 12). A strong coupling material has a higher B_{c2} than one in the weak coupling limit, especially for amorphous materials (ref. 13). Finally, anisotrophy in the Fermi surface greatly enhances (ref. 14) the values of $B_{c2}(0)$. We believe that our samples have an electron phonon coupling constant $\lambda \approx 1$, comparable (ref. 15) to other ternary molybdenum chalcogenides. Therefore, we believe we have a moderately strong coupling material. However, anisotropy and non-dirty limit conditions are viable possibilities. More experiments need to be done to distinguish between these mechanisms.

For the Maki paramagnetic limiting parameter α, the WHH theory gives the relation

$$\alpha = 0.53(-dB_{c2}/dT)_{T/T_c} \tag{1}$$

where B_{c2} and T are in tesla and Kelvin, respectively. From an average slope of about -2.4 tesla/Kelvin one gets $\alpha \approx 1.2$ for our samples. Also from WHH one gets

$$\alpha = 2.35 \times 10^3 \, \rho\gamma \tag{2}$$

where γ is the coefficient of the linear term in the specific heat in Joules/$m^3 K^2$ and ρ is the electrical resistivity in ohm-m. We have measured $\rho \approx 180 \times 10^{-8}$ ohm-m in sample number 118. Thus, $\gamma = 290$ joules/$m^3 K^2$ which is roughly the value found experimentally by Fradin, et al. (ref. 15) for other ternary molybdenum chalcogenides. Thus our value of 1.2 for the paramagnetic limiting parameter, is consistent with other measurements.

Another useful relation (ref. 11) is

$$\kappa = 2.37 \times 10^6 \, \rho\gamma^{1/2} \tag{3}$$

valid in the extreme dirty limit, $\xi \gg l$, where κ is the Ginzburg-Landau kappa. Also

$$\kappa = B_{c2}/\sqrt{2} \, B_c \tag{4}$$

where B_c is the bulk thermodynamic critical field, given by

$$B_c = 7.65 \times 10^{-4} \, \gamma^{1/2} \, T_c \tag{5}$$

So,

$$\kappa = B_{c2}/\left[1.08 \times 10^{-3} \, \gamma^{1/2} \, T_c \right] \tag{6}$$

and by eliminating $\gamma^{1/2}$ from (3) and (6),

$$\kappa^2 = 2.2 \times 10^9 \, \frac{\rho B_{c2}}{T_c} \tag{7}$$

Using experimental values for B_{c2} and T_c, and ignoring variations of κ with temperature yields

$$\kappa \approx 80 \tag{8}$$

From (4) we get the bulk critical field

$$B_c \approx 0.135 \text{ Tesla} \tag{9}$$

From ref. 11:

$$B_{c1} \approx B_x(\ln \kappa + 0.08)/\sqrt{2} \, \kappa \approx 5.3 \times 10^{-3} \text{ Tesla} \tag{10}$$

Thus we have values for the Ginzburg-Landau parameter (10) and all three critical fields, B_{c1}, B_c, and B_{c2}, assuming the dirty limit.

B. Critical Currents and Scaling Laws

As discussed by Ullmaier (ref. 16) and by Campbell and Evetts (ref. 17), one can predict the magnetic field and temperature dependence of the critical current for various models for pinning force densities, P. Pinning force densities are measured by multiplying the critical current density J_c times the value of the field in which J_c was measured (ref. 16). Typical sources of pinning of flux lines are precipitates, dislocations, deformations, grain boundaries, interstitial defects, vacancies, and voids. The results of model calculations for these pinning types can be expressed as

$$P = Df(b)B_{c2}(T)^n/\kappa^m \tag{11}$$

where D, n, m are constants, κ is the Ginzburg-Landau kappa, and f(b) is a function of the reduced magnetic field b only, and not of temperature. κ varies about 20 percent between T_c and 0 K, but we neglect this for the

present. Function f(b) usually is of the form

$$f(b) = b^\kappa (1 - b)^l \qquad (12)$$

where κ and l are constants (ref. 17). Equation (11) is called a "universal scaling" law of experimental results, and if it fits experimental data, it suggests that the same pinning mechanism(s) operate over the entire field and temperature range considered. The usefulness of scaling is that numbers for critical currents at various T's and B's can be found with a limited number of actual measurements.

Critical currents, J_c , were measured as a function of magnetic field at several temperatures, and as a function of temperature in zero field. Measuring J_c in a series of fields at fixed temperatures gives curves such as those plotted in figure 2. Here, b is the reduced field, $B/B_{c2}(T)$. The maximum pinning force for each of the six temperatures shown occurs at $b \approx 0.27$. When these data are replotted by dividing by the pinning force at the maximum, P_{max} , for each temperature, the data fall on nearly a single curve or "scaling" plot (ref. 16) shown in figure 3. In figure 4 we plot the value of the peak pinning force density, P_{max} , for each temperature in figure 2, as a function of critical field $B_{c2}(T)$ on a log-log graph. A straight line results having a slope of ≈ 2.5 . This indicates a value of n = 2.5 in equation (11). From figure 3 we find P/P_{max} data closely follow a dependence

$$P/P_{max} = f(b) \approx b^\kappa (1 - b)^2 \qquad (13)$$

where κ is about 0.6.

Thus,

$$P \propto B_{c2}(T)^{2.5} b^{0.6} (1 - b)^2 \qquad (14)$$

for our samples. The temperature dependence of kappa is still ignored. Since $P = J_c(T) \times B$, and the only temperature dependent part in (14) is $B_{c2}(T)$, then

$$J_c(T) \propto B_{c2}(T)^{2.5} \tag{15}$$

From equation (4), and the "thermodynamic" temperature variation for $B_c(=B_c(0)(1 - t^2))$ (ref. 11) we get

$$J_c(T) = J_c(0)(1 - t^2)^{2.5} \tag{16}$$

Figure 5 shows the good fit of this expression to our data, using our experimental $T_c = 8.2$ K for sample number 181 (representative of group II). This is further evidence for the good applicability of a scaling law (eq. (14)) to our data.

C. Resistivity vs. Temperature

We have measured the electrical resistivity at room temperature and just above T_c in several samples. Typical ratios of these values, ρ_{300}/ρ_{T_c}, are on the order of two, for samples in group II. On sample number 118 (from group I) we find $\rho_{300}/\rho_{T_c} = 4.4$. In addition, we have made very detailed studies of ρ vs. T from T_c to 300 K in number 118. The resistivity is proportional to T^2 from 10 K to 30 K (shown in fig. 6), has an inflection point near 40 K, and has a less than linear dependence on T above 40 K. This behavior of resistivity is qualitatively similar to that found in the high T_c, A-15 structure-materials, and is very different from that in normal metals (ref. 18).

CONCLUDING REMARKS

It would be inappropriate in this paper to make a complete discussion of predictions from various pinning models. It is not likely that we have precipitates as neither the shape of f(b) nor the power 2.5 of $B_{c2}(T)$ allow for

such a mechanism, nor do the electron microscope results support it. However, grain boundaries, a second phase, and probably deformations and dislocations are likely contributors to the pinning force. We do find that a universal scaling law for the critical currents is obeyed. Therefore, we know that the same pinning mechanism(s) hold at all the temperatures. Further work is needed to find out the exact pinning mechanism by changing the sample characteristics.

The magnitude of the pinning force densities are down by about a factor of 50 or less (depending on the reliability of our film thickness measurements) from the best examples existing now for other materials like Nb-Ti (ref. 16). The values of J_c order of magnitude lower than the best commercial Nb_3Sn.

From the critical field vs. temperature data we are able to deduce values for the spin-orbit coupling parameter, α, the paramagnetic limiting parameter λ_{so}, the heat capacity coefficient γ, the Ginzburg-Landau κ, and the critical fields B_{c2}, B_c, and B_{c1}.

REFERENCES

1. R. Chevrel, M. Sergent, and J. Prigent: J. Solid State Chem. 3, p. 515 (1971).

2. B. T. Matthias, et al: Sci. 175, 1465 (1972).

3. R. Odermat, et al.: J. Phys. C. 7, L13 (1974).

4. S. Foner, E. J. McNiff, and E. J. Alexander: Phys. Lett. 49A, 269 (1974).

5. S. Foner, E. J. McNiff, and E. J. Alexander: IEEE Trans. Magnetics MAG-11, 155 (1975).

6. C. Fisher, et al:: J. Phys. C. 8, L474 (1975).

7. C. Fisher: Low Temperature Physics - LT14, M. Krusium and M. Vuorio, eds., (North Holland /American Elseview (Helsinki, Finland, 1975), p. 172.

8. C. Fisher: Physique Sous Champs Magnétiques Intenses (Centre National de la Recherche Scientifique, Paris, 1975), p. 79.

9. C. K. Banks, L. Kammerdiner, and H. L. Luo: J. Solid State Chem. 15, 271 (1975).

10. N. R. Werthamer, E. Helfand, and P. C. Hohenberg: Phys. Rev. 147, 295 (1966).

11. D. Saint-James, E. J. Thomas, and G. Sarma: Type II Super-conductivity (Pergamon Press, New York, 1969).

12. E. Helfand and N. R. Werthamer: Phys Rev. 147, 288 (1966).

13. D. Rainer and G. Bergman: J. Low Temp. Phys. 14, 501 (1974).

14. P. Entel and M. Peter: J. Low Temp. Phys. 22, 613 (1976).

15. F. Y. Fradin, G. S. Knapp, S. D. Bader, G. Cinader, and C. W. Kimball: Electron and Phonon Properties of A-15 Compounds and Chevrel Phases. Submitted to 2nd Rochester Conf. on Superconductivity in d- and f-band Metals. To be published.

16. H. Ullmaier: Irreversible Properties of Type II Superconductors (Springer-Verlag, New York, 1975).

17. A. M. Campbell and J. E. Evetts: Critical Currents in Super-conductors (Barnes and Noble Books, New York, 1972).

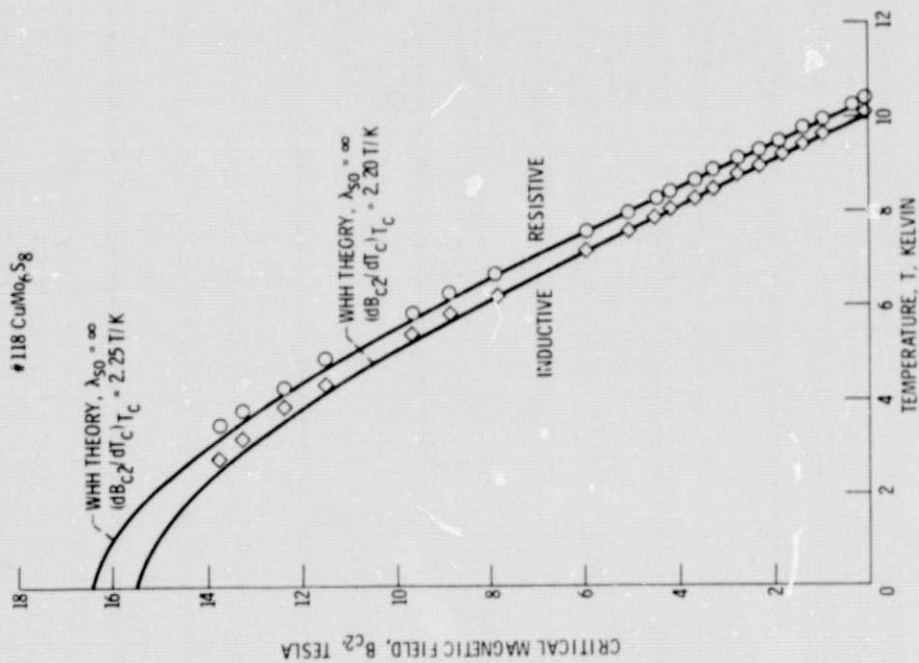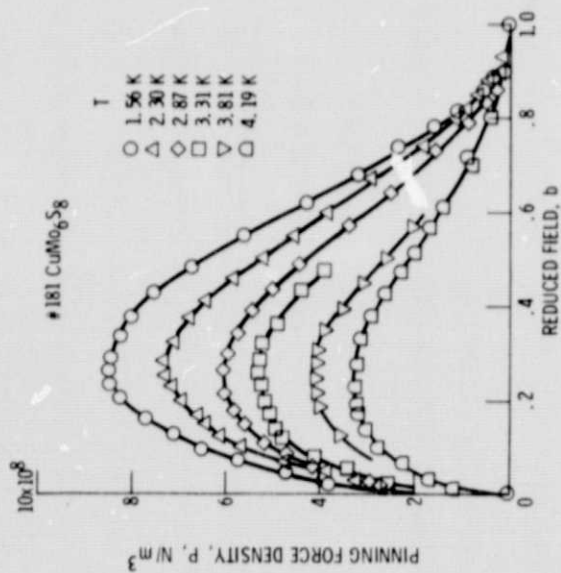18. Z. Fisk and G. W. Webb: Phys. Rev. Lett. 36, 1084 (1976).

Figure 2. - Pinning force density, P, vs. reduced field
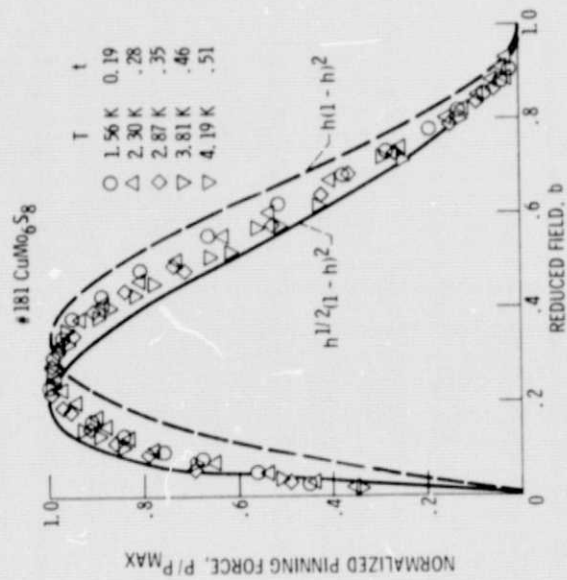b = B/B$_{c2}$, for a series of fixed temperatures for sample
181.

Figure 1. - Critical field, B$_{c2}$, vs. temperature, T, for sample 118.
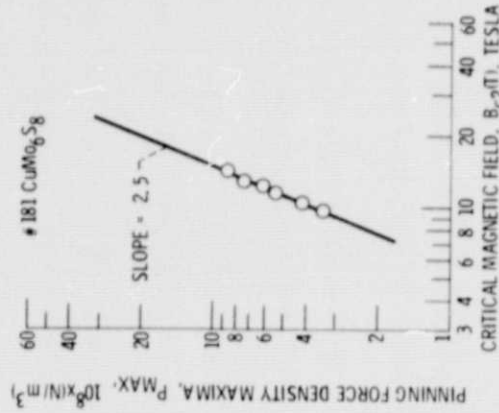Solid lines are from theory (ref. 10).

Figure 4. – Pinning force density maxima P_{MAX} vs. critical magnetic field at several temperatures, $B_{c2}(T)$ for sample 181.

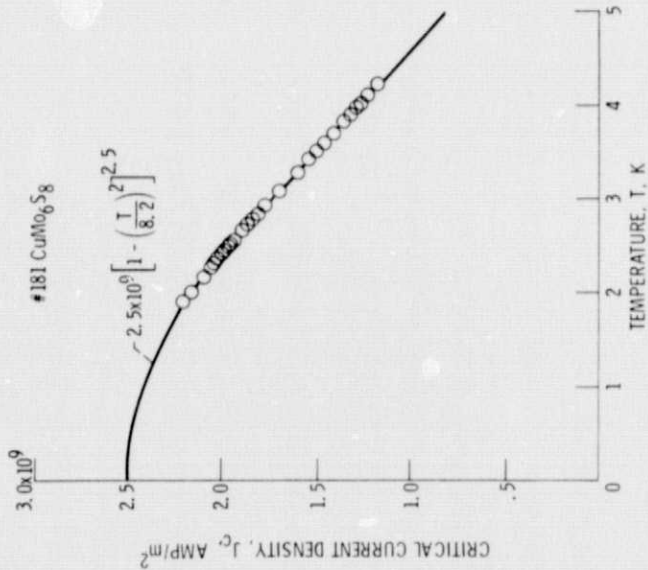Figure 3. – Pinning force density, P, normalized to the value of P at the maximum in figure 2, P/P_{MAX}, vs. reduced field $b = B/B_{c2}$ for the same series of temperatures as in figure 2, and for sample 181.
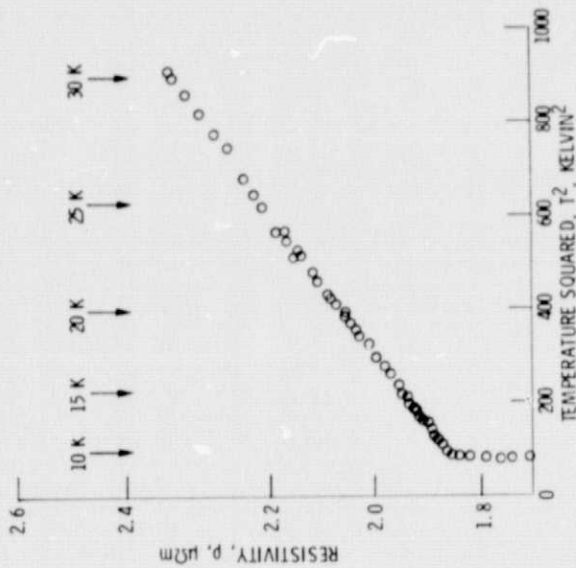
Figure 6. - Normal state resistivity, ρ(T), versus temperature squared, T^2, for sample 118.

Figure 5. - Critical current density, J_C, vs. temperature, T, for sample 181 in zero magnetic field.